Cell Metabolism, Volume *20*

Supplemental Information

Loss of White Adipose Hyperplastic Potential Is Associated with Enhanced Susceptibility to Insulin Resistance

Soo M. Kim, Mingyue Lun, Mei Wang, Samuel E. Senyo, Christelle Guillermier, Parth Patwari, and Matthew L. Steinhauser

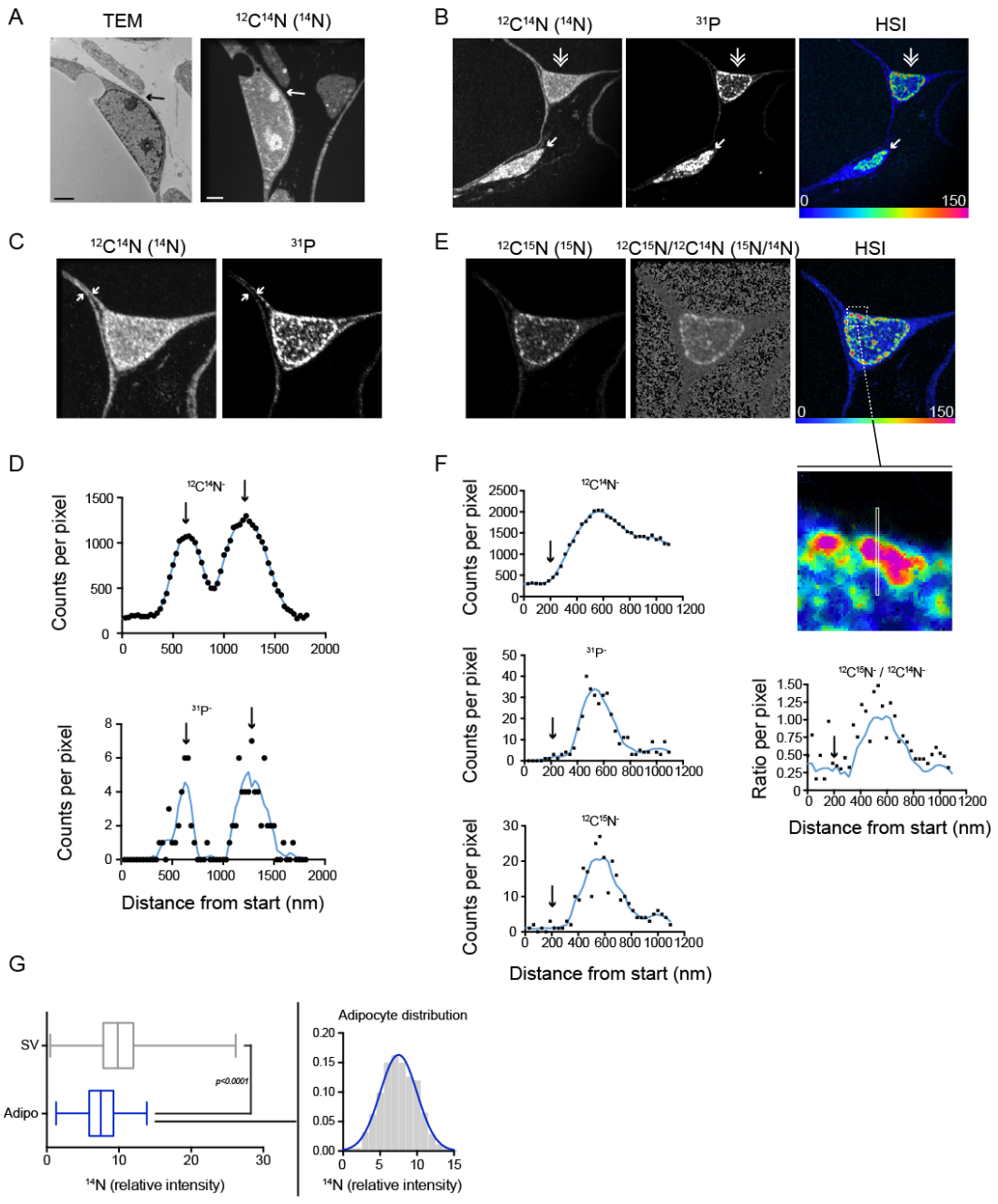

Figure S1 (related to Figure 1). Identifying adipocytes with multi-isotope imaging mass spectrometry (MIMS).

This study utilized qualitative and quantitative aspects of high-resolution MIMS images to distinguish adipocyte nuclei from surrounding interstitial cells. The assignment of adipocyte identify was conducted by a blinded observer. (A) Here, adjacent sections were imaged with transmission electron microscopy (left) and MIMS (right), showing qualitative similarities between

the two methods. The adipocyte nucleus is distinguishable by its close approximation to its defining lipid droplet both contained within the plasma membrane. The arrow shows a sub-micron space between the adipocyte nucleus and an adjacent cell structure in both the TEM image and MIMS image. Scale bar = 2 μm. (B) Shown is an example of an adipocyte nucleus that required additional imaging to verify its identity. The hatched arrow shows the candidate adipocyte nucleus. The small arrow shows a ^{15}N-thymidine labeled interstitial cell. (C) Higher resolution imaging of the adipocyte shown in "B". The white arrows show a region where the plasma membranes of two adjacent adipocytes abut each other. The two adjacent membranes are resolvable visually at this resolution, but can also be identified quantitatively (D) with a line profile taken from a region between the two white arrows. The two peaks (black arrows) correspond to the two adjacent membranes. The ability to rapidly show quantitative line profiles is a feature of the OpenMIMS software (see experimental procedures), which enabled its use in real time by the observer assigning cell identity. Top (D): shows counts of CN^- as a function of distance in nanometers. With this acquisition (512 x 512 pixels, field=16 x 16 μm), the dimensions of each pixel are 31.25 x 31.25 nm. The y-axis represents counts of CN^- ions/pixel. Because of the low ionization efficiency of native nitrogen atoms, nitrogen images are based on measuring CN^- ions. This is made possible by the high mass resolution of the instrument, which distinguishes $^{13}C^{14}N^-$ from $^{12}C^{15}N^-$. Bottom (D): shows the counts of P^-, which are at higher concentrations in phosphor-lipid membranes and the nucleus. (E) Left: Direct measurement of $^{12}C^{15}N^-$ (representative of ^{15}N) is the numerator in the ratio images to the right. The value of the HSI ratio image (far right) provides richer information compared to the grey-scale ratio image (middle), however the underlying quantitative data is not modified by changes in the gray or color scale. For the data collected for this study, the observer assigning adipocyte identity was blind to the data contained in the ratio images. (F) Quantitative line profiles show the close approximation of the lipid droplet (appearing black) to the ^{15}N-labeled nucleus. A region from the lipid droplet / nuclear interface shown in (E) is blown up. Quantitative line profiles are from the vertical white box that is one pixel wide. The inflection point (black arrow at ~ 200nm) in the $^{12}C^{14}N^-$ graph (top) represents the transition from the nitrogen poor droplet to the droplet / nuclear interface. In the same line profile,

there is a slight lag (~100nm) before the increase in P^- counts and increase in the $^{12}C^{15}N^-/^{12}C^{14}N^-$ ratio, consistent with ^{15}N-labeled chromatin. The statistical noise in the first 200nm of the ratio line profile is due to the low counting statistic in the nitrogen-poor lipid droplet. (G) Post-hoc quality control evaluation of the fidelity of adipocyte identification. Different cell types often display different intensities in the nuclear nitrogen signal, presumably due to different degrees of chromatin density and/or protein content. Therefore, the ^{14}N-intensity distribution of a heterogeneous cell population, such as the stromal-vascular fraction (SV) of adipose tissue, does not demonstrate a Gaussian distribution (n=2873). Nuclei identified as adipocytes (n=297), however, are significantly less ^{14}N-intense and segregate into a single Gaussian population shown on the right (Shapiro-Wilk test).

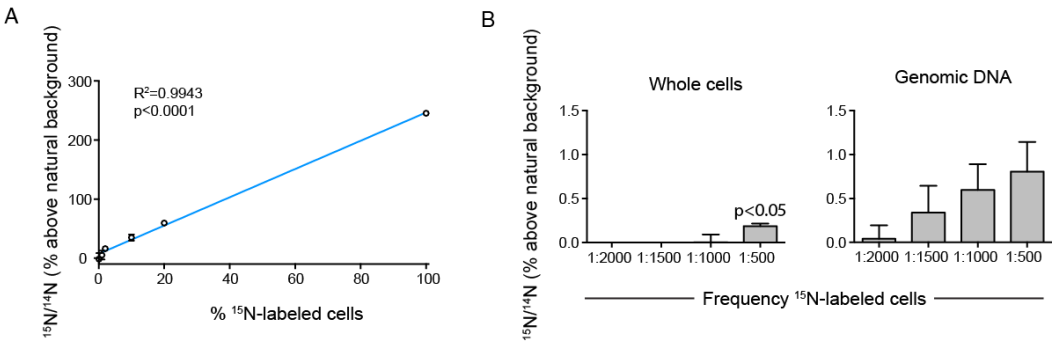

Figure S2 (related to Figure 1). Measuring ^{15}N-thymidine labeled cells with IRMS. 3T3L1 cells were cultured in ^{15}N-thymidine and then mixed at different ratios with unlabeled cells. (A) Linear relationship between ^{15}N-signal and % ^{15}N-labeled cells. (B) Detection of low frequency ^{15}N-labeling, comparing analysis of whole cells or genomic DNA. As expected isolation of genomic DNA strengthens the signal, but we generally observed increased variance of measurements, presumably due to the extra experimental step of genomic DNA isolation. Detection of whole labeled cells was possible down to about 1:500 frequency. Data expressed as mean, ± s.e.m.

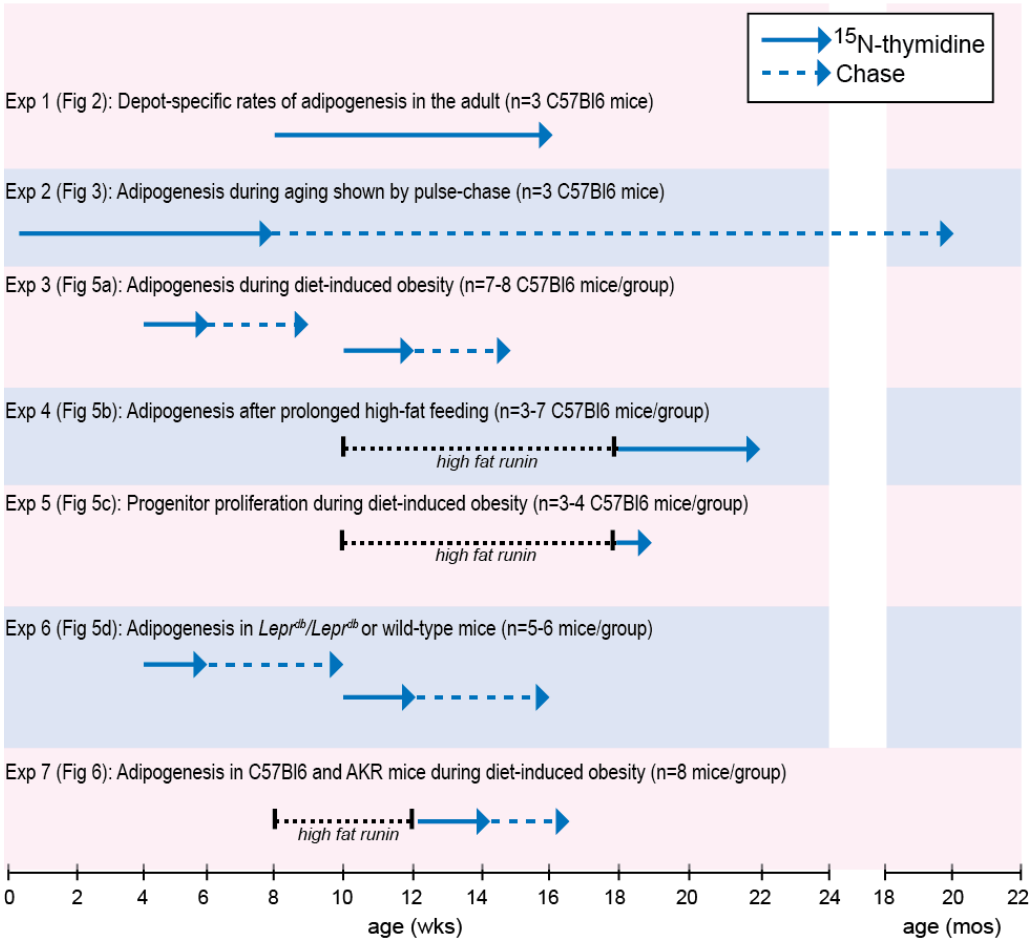

Figure S3 (related to Figures 2,3,5,6). Labeling protocols.

Experiment 1: ^{15}N-thymidine was administered for 8 wks to adult male C57Bl6 mice by osmotic minipump at a continuous rate of 20μg/h.

Experiment 2: ^{15}N-thymidine was administered from post-natal day 4 through week 4 by twice daily subcutaneous injection (50μg/g). At 4 wks, when the mice were large enough, osmotic minipumps were implanted to deliver a continuous rate of 20μg/h through week 8. Mice then underwent an 18-month label-free chase.

Experiment 3: Male C57Bl6 mice, aged 4 or 10 wks, were randomly assigned to normal chow or high fat diet, during ^{15}N-thymidine pulse-chase, which was administered by twice daily subcutaneous injection (25μg/g) for two wks, followed by 3wk label free chase.

Experiment 4: Male C57Bl6 mice, aged 10 wks underwent an 8 wk dietary run-in, receiving normal chow or high fat feeding. They then received ^{15}N-thymidine by osmotic minipump for 4 wks.

Experiment 5: Male C57Bl6 mice, aged 10 wks underwent an 8 wk dietary run-in, receiving normal chow or high fat feeding followed by one wk of ^{15}N-thymidine (25μg/g, twice daily).

Experiment 6: Male *Lepr^{db}/Lepr^{db}* on a C57Bl6SJ background or wild-type (C57Bl6SJ) mice, aged 4 or 10 wks, received ^{15}N-thymidine for 2 wks administered by twice daily subcutaneous injection (25μg/g), followed by 4wk label free chase.

Experiment 7: Male C57Bl6 or AKR mice (8 wks-old) received high fat feeding for 8.5 wks. ^{15}N-thymidine was delivered continuously starting at week 4 for 2 wks. Insulin and glucose tolerance testing was performed after the 8th wk of high fat feeding and the mice sacrificed at 8.5 wks.

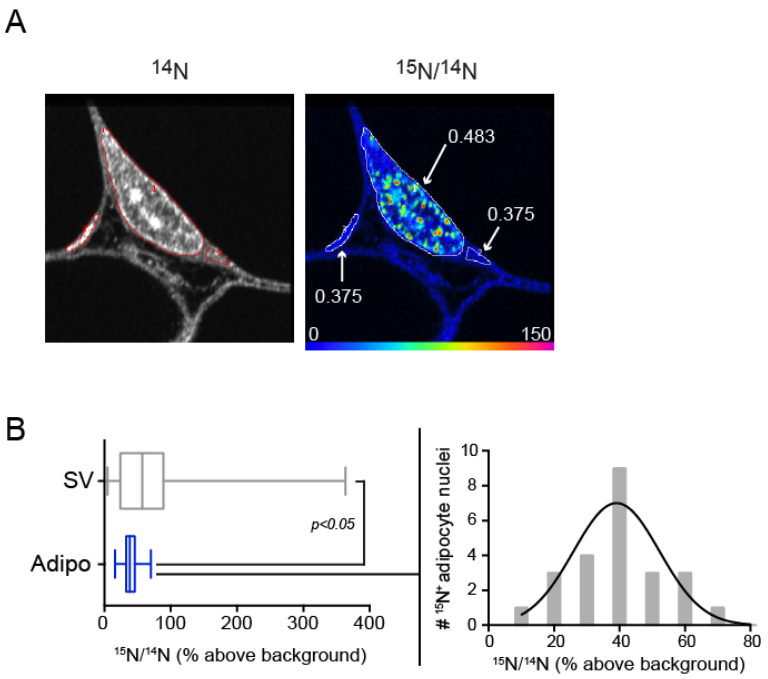

Figure S4 (related to Figure 2). A statistically distinct population of ^{15}N-labeled adipocytes is evident after 8 weeks of continuous ^{15}N-thymidine administration in the adult mouse. (A) Representative ^{15}N-thymidine labeled adipocyte (n= 24). Three regions of interest are shown with their corresponding ^{15}N/^{14}N ratio. Left: small ^{14}N-intense region representing the edge of a nucleus at natural background. Bottom right: region of cytoplasm at natural background. Middle: ^{15}N-labeled nucleus. The rainbow scale ranges from 0-150 % above natural background. (B) ^{15}N-labeled nuclei cluster in a single normally distributed population that is statistically distinct from the skewed distribution displayed by heterogeneous stromal vascular cells that are ^{15}N-thymidine labeled. Cell type specific differences in labeling intensity are likely due to differences in the density of chromatin within the nucleus and/or the result of cells undergoing more than one round of division during the labeling period.

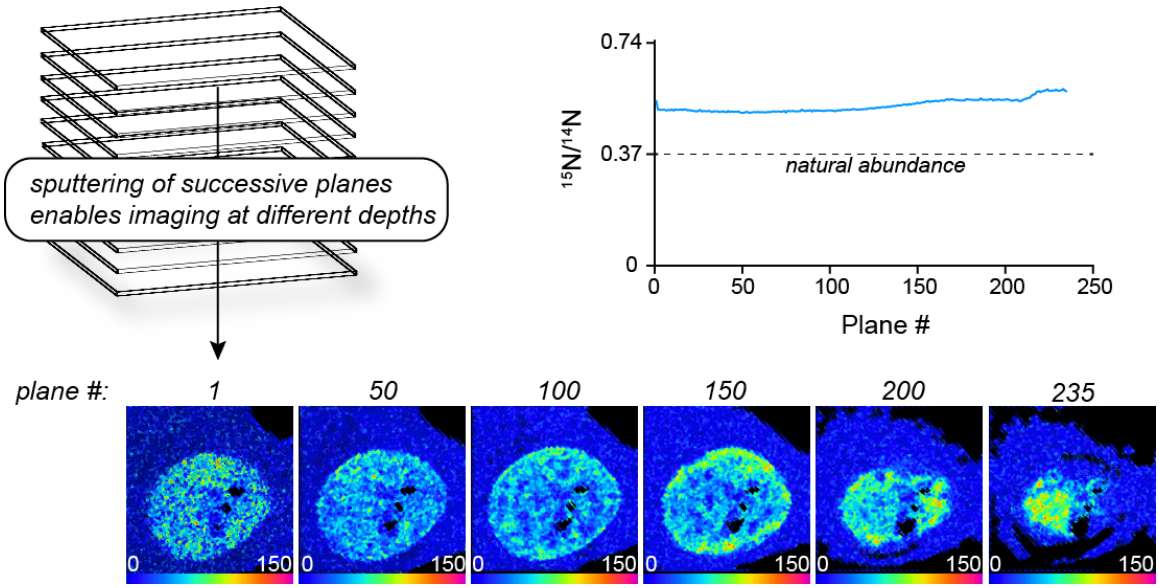

Figure S5 (related to Figure 3). Thin MIMS imaging planes provide a quantitative representation of whole nuclear labeling. 0.5 micron tissue sections were used in this study, but MIMS generates images from a sample volume with a depth dimension as low as a few atomic layers(Lechene et al., 2006; Steinhauser et al., 2012). Shown are representative analytical planes of a fibroblast cultured in ^{15}N-thymidine and subjected to successively deeper measurements. Top right: $^{15}N/^{14}N$ ratio as a function of depth (plane #). The isotope ratio remains quite constant, suggesting that sampling of any given plane provides a quantitative measure of total nuclear labeling, pertinent to quantitative analyses shown in Figure 3. More intense labeling is seen at the periphery of the nucleus, consistent with the tendency of chromatin to condense close to the nuclear membrane and accounting for the subtle increase in isotope ratio at the lower depths of the nucleus shown (between planes 200-235).

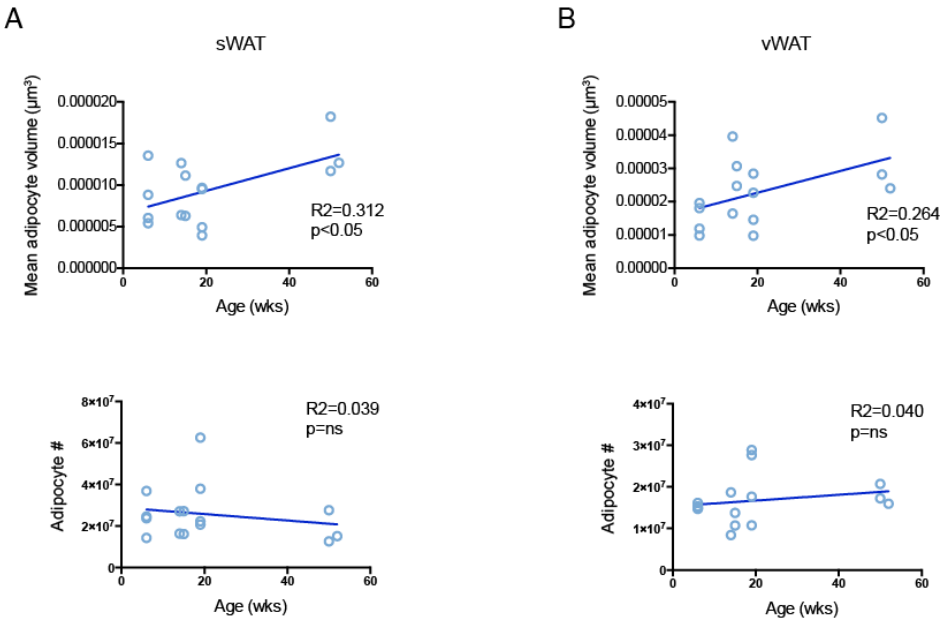

Figure S6 (related to Figure 4). Stability of adipocyte number in adult WAT. Adipocytes were tracked in serial sections. Individual adipocyte volumes were obtained by determining the maximal dimensions of individual adipocytes, using a modification to previously validated methods(Sjostrom et al., 1971). The maximum dimensions of each adipocyte were converted to a volume estimate, assuming sphericity. Total depot volume was calculated by measuring the volume of water displaced by submersion of the excised depot, measurements that as expected were highly correlated with depot mass (R^2=0.953, p<0.0001). Adipocyte number was then calculated by dividing the depot volume by its average adipocyte volume. (A) sWAT morphometrics. Top shows growth of adipocyte volume as a function of age. Bottom: shows no significant change in adipocyte number as a function of age. (B) vWAT morphometrics. Top shows growth of adipocyte volume as a function of age. Bottom: shows no significant change in adipocyte number as a function of age.

Table S1 (related to Figure 4)

	Adipocyte ^{15}N-Positive Proportion (%)		Death Rate (%/week)		Mean Adipocyte Age (weeks)	
	sWAT	**vWAT**	**sWAT**	**vWAT**	**sWAT**	**vWAT**
Actual outcome	73.5	39.2				
Baseline outcome	56.9 (55.4, 58.2)	45.9 (42.7, 48.8)	0.15	2.3	78.9 (78.7, 79.0)	26.9 (26.3, 27.5)
No cell death	56.7 (55.7, 57.6)	53.0 (52.0, 54.1)	0	0	79.1 (78.9, 79.2)	37.2 (37.2, 37.3)
Adipocyte death 50% higher	57.1 (55.5, 58.7)	43.3 (38.8, 48.0)	0.23	3.4	78.8 (78.6, 79.0)	23.6 (22.7, 24.5)
All pre-adipocytes $^{15}N^{+}$	61.2 (60.1, 62.2)	99.6 (99.2, 100.0)	0.15	2.3	78.9 (78.7, 79.0)	26.9 (26.3, 27.6)
Differentiation without division	60.2 (57.5, 62.9)	31.6 (28.7, 34.4)	0.95	7.2	53.2 (52.7, 53.7)	7.88 (7.67, 8.09)
Final model	73.4 (70.9, 75.8)	39.4 (36.6, 42.5)	0.95	3.3	53.2 (52.7, 53.7)	18.3 (17.8, 18.7)

Results of simulation for label-free chase from week 8 until 20 months of age. Results for ^{15}N-positive proportion and adipocyte age are presented as mean (95% confidence interval), calculated by bootstrapping.

Simulation Methods

Overview

We developed a simulation model which takes as input our quantitative experimental data and simulates at a single-cell level ^{15}N label state, birth, death, age, and size. In contrast to previous mathematical models, the extensive quantitative single-cell data allows stochastic simulation by random sampling of probability density functions estimated directly from the observed data. The model includes several parameters that allow testing multiple alternate hypotheses and determining the sensitivity of the outcome to multiple assumptions. All computations were performed in R (v. 3.01, The R Foundation for Statistical Computing, Vienna, Austria). Major methods and assumptions are described below; however, detailed methodology is described within the full source code in R, which is attached as a supplement.

Inputs and Initial Conditions

As input the model used the following observations:

i) SVC ^{15}N label proportions at the beginning and end of Chase
ii) Adipocyte ^{15}N label status and cross-sectional areas at the beginning of the Chase
iii) Adipocyte depot cell number and cell mass over time

Initial cell label proportions were set to the observed proportions for the respective depot at the beginning of the label-free chase. To simulate cell size, the observed cross-sectional areas at the end of the label pulse were used to estimate probability density functions describing cell area for labeled and unlabeled cells in the sWAT and the vWAT. For each simulation run, initial cell areas were then obtained by sampling from the appropriate density function.

Adipocyte Birth and Death

Adipocyte birth rate was given by the birth rate observed during the adult pulse experiment and was assumed to be constant over time. Whether each cell was ^{15}N-positive was determined randomly based on the proportion of ^{15}N-positive preadipocytes in the respective depot. Although the 15N label intensity in the SVC at the beginning of the label-free chase was directly observed, this population is heterogeneous and may underestimate the ^{15}N-positive rate in the progenitor cell population. We therefore included a parameter describing the underestimation rate in each depot. The proportion of labeled progenitor cells was also approximated as decreasing linearly with time over the course of the label-free chase.

Adipocyte cell death was determined stochastically at each time step, with the probability that a given cell dies proportional to the cell's cross-sectional area. The overall cell death rate was modeled as directly proportional the birth rate.

Differentiation without division

In the case that a population of previously labeled progenitor cells differentiate into mature adipocytes without accompanying renewal through division, the rate of ^{15}N-labeled cells observed during the adult pulse experiment will underestimate the overall adipocyte birth rate. We therefore develop an mathematical expression describing the underestimate for use in the model.

First we assume that the overall adipocyte birth rate is a constant, *g*. Then the rate of change of the total number of adipocytes *N* is given by:

$$\frac{dN}{dt} = g$$

So for t > 0, and N(t=0) = N_0, *N(t)* is given by:

$$N(t) = g\,t + N_0$$

However, the number of observed $^{15}N^+$ adipocytes immediately following a ^{15}N-thymidine pulse only gives *g* directly if all new adipocytes form by differentiation of dividing preadipocytes. If some new adipocytes form by differentiation of existing pre-adipocytes without further division, not all new adipocytes will be labeled $^{15}N^+$. The rate of formation of ^{15}N-negative adipocytes can be described as the product of the fraction of preadipocytes that are unlabeled, $f_{SVC-}(t)$, and the fraction of the overall adipocyte birth rate that proceeds by differentiation without division, f_{DS}. The rate of change of ^{15}N-positive cells is then:

$$\frac{dN_{15N+}}{dt} = g - f_{SVC-}(t)\,f_{DS}\,g$$

Modeling the increase in the labeled fraction of the SVC compartment as linear over time for the 8-week pulse, we let $f_{SVC+}(t) = at$, where $a = f_{SVC+}(t = 8\ wks)/8\ wks$. Then

$$\frac{dN_{15N+}}{dt} = (1 - f_{DS})\,g + f_{DS}\,a\,g\,t$$

Integration gives

$$N_{15N+} = (1 - f_{DS})\,g\,t + \frac{1}{2}a\,g\,t^2$$

Solving for the fraction of ^{15}N-positive adipocytes observed at t > 0 yields

$$\frac{N_{15N+}(t)}{N(t)} = \frac{(1 - f_{DS})\,g\,t + \frac{1}{2}(f_{DS})\,a\,g\,t^2}{g\,t + N_0}$$

Finally, solving for the true birth rate *g* based on the observed data at *t* = 8 weeks:

$$g = \frac{\frac{N_{15N+}(t=8)}{N(t=8)}}{8\left[(1 - f_{DS}) + \frac{1}{2}f_{DS}\,f_{SVC}(t=8)\right]}N_0$$

Model Output

The final mean adipocyte ^{15}N label proportion and adipocyte age were recorded directly from the simulation. Adipocyte lifetime over this time period was heavily censored, but was estimated by the average lifetime of cells that died at the end of the chase. 95% confidence intervals for the mean values were generated by bootstrapping from the simulation results.

Simulation Results

All reported results are for at least 1000 independent runs of 1000 cells in each depot simulated over 18 months in 40 time steps. Increasing these numbers further had little effect on the model results and confidence intervals.

The results of the final model that fit the observed proportion of $^{15}N^{+}$ cells at the end of the label-free chase are given in Table S1. In addition the estimated mean adipocyte lifetime was 70.3 (60.3, 78.9) weeks in the sWAT and 30.1 (26.7, 34.2) weeks in the vWAT. The parameters for the final model were as follows:

i) birth and death rate equal and constant over time

ii) preadipocyte label proportion underestimate of 56% in the sWAT and 0% in the vWAT

iii) fraction of adipocyte birth by differentiation without progenitor cell division of 100% in the sWAT and 46% in the vWAT

Supplemental References

Lechene, C., Hillion, F., McMahon, G., Benson, D., Kleinfeld, A.M., Kampf, J.P., Distel, D., Luyten, Y., Bonventre, J., Hentschel, D.*, et al.* (2006). High-resolution quantitative imaging of mammalian and bacterial cells using stable isotope mass spectrometry. J Biol *5*, 20.

Sjostrom, L., Bjorntorp, P., and Vrana, J. (1971). Microscopic fat cell size measurements on frozen-cut adipose tissue in comparison with automatic determinations of osmium-fixed fat cells. J Lipid Res *12*, 521-530.

Steinhauser, M.L., Bailey, A.P., Senyo, S.E., Guillermier, C., Perlstein, T.S., Gould, A.P., Lee, R.T., and Lechene, C.P. (2012). Multi-isotope imaging mass spectrometry quantifies stem cell division and metabolism. Nature *481*, 516-519.